Journal of Environmental Sciences
March 2021, Volume 101 Pages 313-325
https://doi.org/10.1016/j.jes.2020.08.027
https://archimer.ifremer.fr/doc/00648/76028/

Trace metal dynamics in an industrialized Brazilian river: A combined application of Zn isotopes, geochemical partitioning, and multivariate statistics

Tonhá Myller S. [1, *] , Ferreira Araujo Daniel [2], Araújo Rafael [1], Cunha Bruno C.A. [3], Machado Wilson [4], Portela Joelma F. [5], Pr Souza João [5], Carvalho Hikari K. [1], Dantas Elton L. [1], Roig Henrique L. [1, 6], Seyler Patrick [3, 7], Garnier Jeremie [1, 6]

[1] Universidade de Brasília, Instituto de Geociências, Campus Darcy Ribeiro, L2, Asa Norte, 70910900 Brasília, Distrito Federal, Brazil
[2] Laboratoire de Biogéochimie des Contaminants Métalliques, Ifremer, Centre Atlantique, F44311 Nantes Cedex 3, France
[3] Institute of Geosciences, University of São Paulo, Rua do Lago, 562, São Paulo 05508-080, Brazil
[4] Universidade Federal Fluminense, Programa de Geoquímica, Campus do Valonguinho, Niterói, Rio de Janeiro, Brazil
[5] Analytical and Environmental Chemistry Laboratory, Instituto de Química, University of Brasilia, Brasilia, Federal District 70919-970, Brazil
[6] Laboratoire Mixte International “Observatoire des Changements Environnementaux” (LMI OCE), Institut de Recherche pour le Développement/University of Brasilia, Campus Darcy Ribeiro, Brasilia, Brazil
[7] Hydrosciences Montpellier, Université de Montpellier, Institut de Recherche pour le développement, Centre National de la Recherche Scientifique, Montpellier, France

* Corresponding author : Myller S. Tonhá, email address : myller@unb.br

Abstract :

The Paraiba do Sul (PSR) and Guandu Rivers (GR) water diversion system (120 km long) is located in the main industrial pole of Brazil and supplies drinking water for 9.4 million people in the metropolitan region of Rio de Janeiro. This study aims to discern the trace metals dynamics in this complex aquatic system. We used a combined approach of geochemical tools such as geochemical partitioning, Zn isotopes signatures, and multivariate statistics. Zinc and Pb concentrations in Suspended Particulate Matter (SPM) and sediments were considerably higher in some sites. The sediment partition of As, Cr, and Cu revealed the residual fraction (F4) as the main fraction for these elements, indicating low mobility. Zinc and Pb were mostly associated with the exchangeable/carbonate (F1) and the reducible (F2) fractions, respectively, implying a higher susceptibility of these elements to being released from sediments. Zinc isotopic compositions of sediments and SPM fell in a binary mixing source process between lithogenic (δ66/64ZnJMC ≈ + 0.30‰) and anthropogenic (δ66/64ZnJMC ≈ + 0.15‰) end members. The lighter δ66/64ZnJMC values accompanied by high Zn concentrations in exchangeable/carbonate fraction (ZnF1) enable the tracking of Zn anthropogenic sources in the studied rivers. Overall, the results indicated that Hg, Pb, and Zn had a dominant anthropogenic origin linked to the industrial activities, while As, Cr, and Cu were mainly associated with lithogenic sources. This work

demonstrates how integrating geochemical tools is valuable for assessing geochemical processes and mixing source effects in anthropized river watersheds.

Graphical abstract

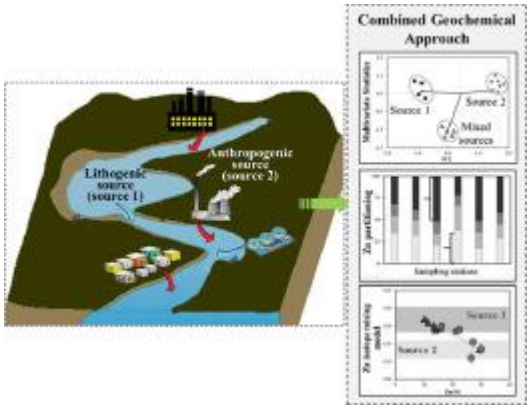

Keywords : Metal pollution, Isotope tracer, Sequential extraction, Anthropogenic activity

Introduction

Rivers are ecosystems of upmost importance for human life as primary sources of drinking water. However, intensification of industrialization and urbanization processes in river watersheds worldwide threat the fluvial water quality (Zhao et al., 2018). In particular, trace metals contamination is of great concern because of these chemical species' persistent behavior, and once they are introduced in the aquatic medium, they become susceptible to incorporation by biota and ultimately by humans.

Sorption processes involving high-charged surfaces of fine particles, such as clay minerals, Fe and Mn oxyhydroxides, organic matter, or (co-)precipitate as sulfides, carbonates or oxides control the dispersion, transport, and remobilization of trace metals (Zhang et al., 2014). In turn, speciation determines the bioavailability and toxicity of metals, which are properties governed by environmental conditions (e.g., ionic strength, pH, redox, and organic matter) and biological activity (Hahn et al., 2018). The multiplicity of biogeochemical factors involved in the dynamic of trace metals in aquatic systems makes environmental and health risks assessment challenging.

To elucidate the behavior and risk of these chemical species in complex aquatic systems, selective extraction procedures (SEP) have been employed to provide knowledge about partition, potential mobility, and bioavailability of trace metals (Du Laing et al., 2009). The SEP protocol developed by the Bureau Communautaire de Reference (BCR) (Rauret et al., 2000) allows the trace metals partitioning determination in riverine sediments polluted by industrial effluents (Gao et al., 2018), steel wastes (Mäkelä et al., 2015), and metallurgical leach residues (Sethurajan et al., 2016). Furthermore, non-traditional isotope systems, notably the zinc isotopes, have been successfully applied as tracers of anthropogenic emissions and low-temperature biogeochemical processes in large river basins (Chen et al., 2009b; Desaulty and Petelet-Giraud, 2020; Petit et al., 2015; Zimmermann et al., 2020). Zn isotope compositions (expressed as $\delta^{66/64}Zn_{JMC}$ notation) are used as source identification tools (Araújo et al., 2017a; Li et al., 2019; Tonhá et al., 2020; Xia et al., 2020), which can distinguish between lithogenic materials derived from weathering processes (+0.28 ± 0.05 ‰) (Chen et al., 2013) and anthropogenic materials, such as road dust (+0.08 to +0.17 ‰) and tire-wear (+0.00 to +0.22 ‰) (Dong et al., 2017; Souto-Oliveira et al., 2019).

The Paraiba do Sul (PSR) and Guandu Rivers (GR) water diversion system constitute a complex hydrological feature affected by the main Brazilian industrial park and multiple land-use activities (e.g., industries, farm, irrigation, sand exploitation, water reservoirs, drinking water, and river channelization) (Britto et al., 2016). Since the 1950s, two-thirds of the PSR water is diverted to the GR to supply drinking water for more than 9.4 million inhabitants of the metropolitan region of Rio de Janeiro (MRRJ) and to furnish raw water to industrial plants (Miguens et al., 2016). However, some studies concerning metal contaminations in this area reported high metal concentrations (Cd, Cr, Cu, Pb, Ni, and Zn) in the dissolved, particulate and sediment phases (Barcellos and Lacerda, 1994; Molisani et al., 2006; Pfeiffer et al., 1986; Valitutto et al., 2007). Santos-Neves et al. (2018) were the first to consider the speciation of dissolved metals (rare-earth elements), as affected by Fe and Mn oxyhydroxides co-precipitation and biological uptake in the GR water reservoirs.

The PSR-GR is an environment impacted by multiple diffuse source pollutants and was considered a strategical system to test the complementary use of geochemical tools for tracing metal sources, partitioning, and ecological risks assessment. To date, the anthropogenic origins of trace metals and its geochemical behavior along this diversion system remain unclear. Nevertheless, few geochemical studies have coupled SEP with Zn isotopic signatures to assess trace metal sources (Resongles et al., 2014; Thapalia et al., 2010).

To better understand the dynamic of trace metals in the PSR-GR system, the present study combines elemental concentrations in dissolved, suspended particulate matter (SPM), and surficial sediment samples with chemical partitioning and Zn isotope information of solid phase. Based on a prior study reporting Zn contamination, the use of Zn isotopes is of particular interest to track sources and fates (e.g., Pfeiffer et al., 1986). The association of these geochemical tools was used to (1) assess the enrichment of trace metals (As, Cd, Cr, Cu, Hg, Zn, Pb), (2) evaluate the partition in sediment phase and associated environmental risk, and (3) characterize anthropogenic sources of metals and their transport along the watershed.

1 Methods

1.1 Study area

The Paraiba do Sul (PSR) and Guandu Rivers (GR) watershed is situated at the southeast of Brazil and flows through São Paulo and Rio de Janeiro states (**Fig. 1**). The PSR is 1145 km long, drains 56,600 km^2, and discharges into the South Atlantic at 22 °S latitude. The GR basin covers 1500 km^2 and the main uses of its water is human consumption (80%) (treated in the second biggest water treatment plant of the world), industrial demands (2.4%), and other activities (17.6%) (Santos-Neves et al., 2018). The GR discharge represents about 86% of the total fluvial inputs into the coastal lagoon of Sepetiba Bay. The amounts of water and SPM reaching Sepetiba Bay have been drastically altered by the water diversion from the PSR, corresponding to increases of 88 $m^3 s^{-1}$ and 270 t yr^{-1}, respectively (Molisani et al., 2004). Marins et al. (1998) appointed the GR as the main fluvial source of dissolved and particulate Hg for Sepetiba Bay, a lagoon estuary located at the outlet of GR.

The basin drained by the PSR (R1 site, **Fig. 1**, **Table S1**) consists of metamorphic (gneissic banding, schists, amphibolite, marble, calc-silicate, and granulites) and silicate (quartzite, biotite, garnets) rocks of Paraíba do Sul and Juiz de Fora complexes from the Neo and Paleo Proterozoic ages, respectively (CPRM - Geological Survey of Brazil, 2000). Downstream, after the diversion system from PSR to GR (R2 site), igneous rocks (granite, foliated granodiorite, and autolytic quartz diorite) from the Quirino Suite of the Paleoproterozoic occurs. The transposed waters of the PSR are then diluted with the waters of the preserved Piraí River to form the Vigario reservoir, followed by the Nilo Peçanha hydroelectric plant and the Ponte Coberta reservoir. The R3 site is situated downstream of these reservoirs. The geology of this point displays igneous rocks (S-type peraluminous granitoid) of the Araçuaí-Rio Doce orogen

129 from the pre- to synorogenic magmatism of the Paleozoic. The Piraí River shows the same
130 complexes of the R1 site (Paraíba do Sul and Juiz de Fora). In the downstream direction, the
131 R4 site, situated under the main Brazilian highway (BR116) and near two thermoelectric power
132 plants, is composed of the Rio Negro Magmatic Arc from Neoproterozoic with Quaternary
133 fluvial-lacustrine deposits. Lastly, the R5 (near a water treatment plant - WTP) and R6 (6 km
134 upstream to the river mouth in the Sepetiba Bay) sites are formed by Quaternary fluvial-
135 lacustrine deposits too.

136 Since the middle of the 20th century, intense industrial activities have inputted high
137 contents of metals into both rivers. There are more than 6500 industrial plants registered in the
138 PSR watershed (upstream to the R1 site), such as metallurgical, steel, chemical, and
139 petrochemical plants, but it is estimated that only 64 of these account for more than 81% of the
140 total pollutant load (Molisani et al., 2004). These include two large iron and steel plants
141 (*National Steel Company* - SCN, the largest steel producer in Latin America - and *Guanabara*
142 *Steel Company* - COSIGUA); 19 pyrometallurgical smelters (> 33,000 t y^{-1} production),
143 including Quimvale industry; 16 chemical plants (Molisani et al., 2004); and two gas-fired
144 power plants (thermoelectric) (**Fig. 1**). Moreover, the urban area of MRRJ, a sewage treatment
145 plant, and sand mining (Marques et al., 2012) may also contribute to the enrichment of metals.

146

147 **1.2 Sampling and sample preparation**

148 This study considered six representative sampling sites, chosen according to previous
149 studies, to investigate the most relevant geochemical process of the PSR-GR (Molisani et al.,
150 2006; Valitutto et al., 2007). Sampling was conducted in June 2017 during the wet season. From
151 upstream to downstream along the PSR-GR, the sites are (**Fig. 1** and **Table S1**): Paraiba do Sul
152 River before diverted waters (R1), Santa Cecília (R2), Ponte Coberta (R3), BR-116 road (R4),
153 water treatment plant (R5) and São Francisco Channel (R6). The sampling encompassed waters
154 (N = 6), surficial sediments (N = 6), surficial soil (N = 1), and a granite rock (N = 1), where
155 "N" is the number of samples. The samples were identified with the codes of the respective
156 sampling station followed by an abbreviation of the sample matrix type: water (w), suspended
157 particle material (SPM), surficial sediment (sed), soil (s), and rock (r). The soil sampled in the
158 R3 site was classified as fluvisol (IUSS Working Group WRB, 2014).

159 The surficial sediments were collected at a 0-3 cm depth using a Van Veen grab sampler
160 and the soil was collected using a plastic shovel. All samples were preserved in ice-packed

boxes for further preparation in the laboratory. The surficial sediments and soils were air-dried, crushed, homogenized, and sieved in two fractions: < 2 mm for sediment grain size distribution and soil analyses; and < 63 μm for mineralogy, Hg, elemental, sequential extraction and isotopic analyses of sediments. Granite rock sample was pulverized in a mill with agate balls.

Surficial water was collected at an ~1m depth with a Van Dorn bottle, stored in 1L precleaned low-density polyethylene (LDPE) bottles, and preserved in ice-packed boxes for further filtrations in the laboratory. In the laboratory, the water samples were filtered through acid-cleaned (5% HNO_3, Merck) and previously weighted 0.22 μm mixed cellulose ester (MCE) membrane filters (Millipore®).

1.3 Analytical procedures

Complementary laboratory methods, such as physicochemical parameters, dissolved anions, carbon analysis, and solid characterization of sediments (Total organic carbon and X-ray diffractometry) are described in supplementary data. All procedures, including the digestion and evaporation steps, were carried out in a 1000 class cleanroom. Dilutions were performed using high-purity water (>18.2 MΩ) produced by a Milli-Q (Nanop System®).

The solid samples (sediments, soil, SPM, and rock) were weighed in a Savillex® PFA vials and digested in two independent replicates on a hot plate using a multiple-step double-distilled acid procedure with HF, HNO_3, H_2O_2, and HCl (Merck). The final solid was redissolved with 10 mL of HCl 2 M and centrifuged for further analysis. The partition of metals associated with acid-soluble (F1), reducible (F2), oxidizable (F3, and residual (F4) solid phases was obtained using the extraction protocol of the European Community Bureau of Reference, here labeled "BCR" (Rauret et al., 2000). The extractions were performed in three independent replicates using suitable chemical reagents purchased from Sigma Aldrich (Canada).

The concentrations of elements were determined by ICP-OES (5100, Agilent, USA) and ICP-MS (Q-Thermo Scientific, USA). Total Hg in sediments and SPM samples were analyzed using TD-AAS (Lumex Instruments, RA915+, USA). Analytical blanks were determined according to the recommendation of Rauret et al. (2000), i.e., resulting in values lower than the L.D. of analysis. For analytical control, the following certified reference materials were used: NIST (San Joaquin Soil SRM 2709a and Estuarine sediment 1646a) for total metals concentration after digestion; NRC (SLRS-5) and Mississipi-03 (CRM Environment Canada)

for water analysis; and BCR-701® (Freshwater Lake Sediment) for BCR extraction (**Table S2**). The accuracy of the reference materials averaged within ± 5% of certified values. The relative standard deviations (RSD) of the replicates in elementals and SEP analysis was around ±10%.

1.4 Zinc isotope analysis

The analysis of Zn isotopic ratios was carried out on all surficial sediments, soil, rock, and SPM. An aliquot of the sample containing about 2 µg of Zn was purified by anion exchange chromatography (2 mL of Biorad AG-MP1) according to an adapted protocol from Maréchal et al. (1999). The quantitative recovery of the purification process (±10%) was checked by ICP-OES, and the procedure blanks (1 ng) were < 1% of the Zn mass content of the samples (2 µg). Isotopic analyses of purified Zn samples were performed using MC-ICP-MS (Neptune, Thermo Scientific, Germany) at the Geochronology Laboratory at the University of Brasília (Brasília, Brazil). Purified samples were redissolved in 2% (v/v) HNO_3 and introduced in the MC-ICP-MS equipment with a stable injection system (SIS: cyclonic spray chamber) coupled with a low flow PFA nebulizer (50 µl min^{-1}). The masses ^{62}(Ni), ^{63}(Cu), ^{64}(Zn/Ni), ^{65}(Cu), ^{66}(Zn), ^{67}(Zn), and ^{68}(Zn) were simultaneously detected using Faraday cups (for more details see Araújo et al., 2017b). The instrumental mass bias was corrected by Cu doping NIST-SRM 976 (Zn:Cu 1:1, m/m) and using the standard-sample bracketing technique combined with external normalization and exponential law. All Zn isotopic results are expressed as $\delta^{66/64}$Zn reported to JMC-Lyon (Johnson Matthey Company, lot 3-0749-L):

$$\delta^{66/64}Zn_{JMC}(‰)=\left(\frac{R(^{66}Zn/^{64}Zn)_{sample}}{R(^{66}Zn/^{64}Zn)_{JMC}} - 1\right)*1000 \quad (1)$$

The $\delta^{66/64}Zn_{JMC}$ of reference materials IRMM3702 (+0.32 ± 0.02, 2 s, n = 6) and BHVO-2 basalt (+0.28 ± 0.01 ‰, 2 s, n = 5, where "n" is the number of replicates) were measured during the analytical session to assess the analytical control of the chromatographic procedure and of the analytical session itself. The results were close to the $\delta^{66/64}Zn_{JMC}$ reported by Moynier et al. (2017). Full replicates (including subsampling, digestion, chromatographic separation, mass spectrometry) for bulk samples fell within the average analytical reproducibility obtained on reference materials. The average external reproducibility (2 s) of the method was ± 0.06 ‰, determined from replicates of reference materials. The uncertainty bars reported in the figures

correspond to the external reproducibility. These values are indistinguishable from previous measurements conducted for over five years according to the same analytical sequences and performed in various laboratories (Araújo et al., 2017a; Araújo et al., 2017b; Araújo et al., 2018; Souto-Oliveira et al., 2019; Araújo et al., 2019a).

1.5 Enrichment factors for the surficial sediment

The enrichment factor (EF) was used to estimate anthropogenic metal inputs and to minimize the influence of grain size and dilution effects on the metals concentrations in sediments, according to Eq. (1).

$$EF = (M/Ti)_{sample}/(M/Ti)_{background} \quad (2)$$

where $(M/Ti)_{sample}$ and $(M/Ti)_{background}$ are the concentration ratios of a given metal in the unknown sediment sample and the representative background sediment sample (R0), respectively (see **Fig. 1** in the lower right rectangle). This sediment background was collected at the Paraíba do Sul spring, located 300 km upstream from the R1 site (**Table S1**). Titanium was selected as a conservative element to calculate the enrichment factor (EF) since it was mostly associated with lithogenic sources (Sutherland 2000). The EF values were classified as suggested by Chen et al. (2007): EF < 1 is not enriched; 1 < EF < 3 is slightly enriched; 1 < EF < 5 is moderately enriched; EF > 10 is moderately to severely enriched.

1.6 Statistical analysis

Statistical analysis was carried out in the Statistica software version 13.3, where the principal component analysis (PCA) was used to reduce the dataset information and hence, assist the geochemical interpretation. The PCA was carried out with Varimax rotation and retention of principal components whose eigenvalues were greater than unity. The variables normality was determined through the Kolmogorov–Smirnov test. Student's t-test (T) for variables with normal distribution and the Mann–Whitney test (U) for variables with non-normal distribution were used for mean comparisons between the sites and literature results. Pearson's correlation was used to test the relationship between variables. A probability level

(p) below 0.05 was considered statistically significant. Values were expressed as the mean ± standard error.

2 Results

2.1 Main properties of dissolved phase

The average concentrations of trace metals in the dissolved phase follows the order Zn > Cu >> Cr ≈ As ≈ Pb > Cd (**Fig. 2a**, **Table 1**, and **Table S5**). Other results of the dissolved phase such as physicochemical parameters (pH, EC, and dissolved oxygen), major anions, and major cations are shown in the Supplementary Material (**Table S4**). All range of concentrations related to dissolved trace metals are compiled in **Table 1**, as well as those observed in previous studies in the same area, in other regions, and World Health Organization (WHO) (WHO, 2017) and USEPA (USEPA, 2000) guidelines.

2.2 Elemental concentrations and mineralogical characterization of sediments and soils

The average SPM concentrations of trace metals follows the order Zn >> Cr > Cu ≈ Pb >> As > Cd (**Fig. 2c**, **Table 1**, and **Table S7**). Along the path of the studied rivers, the maximum concentration of Cr, Pb, and Zn in SPM is observed in the R1, R2, and R4 sites. The X-ray diffractograms patterns of SPM show peaks attributed to crystalline phases, mainly for gibbsite and clay minerals (kaolinite and muscovite) (**Fig. S1a**). The mineralogy of the samples is homogeneous and **Fig. S1a** shows a typical diffractogram (R1 SPM).

The results of total metal concentrations and ranges in sediments and soils are given in **Fig. 2e**, **Table 1**, and **Table S9**. The metals concentrations averages in sediments and soil follow this order: Zn > Cr > Cu ≈ Pb > As > Cd > Hg. The mineralogy of surficial sediments is composed mainly of quartz, K-feldspar, gibbsite, and clay minerals (kaolinite, illite, and muscovite) (**Fig. S1b**). The mineralogical pattern of surficial sediments is uniform and can be represented by the R1 sediment sample in **Fig. S1b**.

2.3 Principal Component Analysis

The PCA exploratory approach for the water data is presented in **Fig. 2b**. The dissolved fraction variables correlate with two principal components (PCs), representing 66% of the total

variance. The first factor (PC1), representing 51% of the total variance, has a high factor loading for variables Na^+, Cl^-, NO_3^-, and SO_4^{2-}, and was positively correlated to the R1, R2, and R6 sites (R1 > R2 > R6). The second factor (PC2), which accounts for 15% of the total variance with high factor loading for Cr and Zn, is associated with the R6 site. The Cu, Fe, Al, and DOC variables show negative factor loadings with the variables of PC1, and were positively associated with R5 and R3 sites (R5 >> R3).

The PCA of the SPM dataset yields two principal components accounting for 77% of the total variance (**Fig. 2d**). The PC1 contributes with 58% of the total variance, showing high factor loadings for As, Cr, Cu, Pb, and Zn, and is associated with R1, R4, and R2 sites (R1 > R4 > R2). The factor loads of major elements (Fe, Mn, Ti, Al, and Ca) and the scored of the R3 site are anti-correlated to the R3 and R5 sites (cluster in **Fig. 2d**). The PC2 accounted for 19% of the total variance, which was anti-correlated to the R6 site and cadmium. The PCA of the SPM phase showed a grouping of POC and suspended trace metals (**Fig. 2d**). Furthermore, it was observed a high correlation ($p < 0.05$) between suspended Al and Fe, and suspended trace metals, e.g., Zn x Fe ($r^2 = 0.97$), Zn x Al ($r^2 = 0.95$), Pb x Fe ($r^2 = 0.98$), and Pb x Al ($r^2 = 0.89$).

The PCA of sediment data breaches into two principal components (**Fig. 2f**), with 71% of the total variance. The PC1 (49%) shows high factor loadings for Cr, Cu, Hg, and Al, and are grouped with the R3 site. Despite the variables Fe and Mn not being grouped with the R3 site, they present considerable factor loadings (> 0.60) in the PC1. The variable P correlates with R5, R2, and R1 sites and shows negative factor loading to PC1 (R5 > R2 > R1). The PC2 (22%) shows positive factor loading for As, correlating to the R1 site, and negative factor loadings for Pb and Zn, correlating to the R4 site.

2.4 Trace metal partition in sediments

The BCR extraction data for As, Cd, Cr, Cu, Pb, and Zn in surficial sediments (N = 6) are displayed in **Fig. S3**, **Table 2**, and **Table S10**. All metals were preferentially associated with the residual fraction (F4), but the overall partition differs among the sediment phases. Zinc was preferentially associated with this fraction (ZnF4 = 39 ± 11%) and the remaining percentage was mostly distributed in the exchangeable/carbonate (ZnF1 = 29 ± 8%). The BCR results of the R4 site show a higher percentage of Zn associated with F1 (39%) and F2 (27%) fractions. The partition of Pb was dominated by reducible (PbF2 = 53 ± 10%) and residual

(PbF4 = 36 ± 13%) fractions. The partition of Cu was more abundant in the residual (CuF4 = 47 ± 4%) and oxidizable (CuF3 = 26 ± 4%) fractions.

2.5 Zn isotope compositions of sediments and SPM

The Zn isotope compositions of rock, soil, SPM, and sediments are given in **Table 2** and **Fig. 3**. The $\delta^{66/64}Zn_{JMC}$ values ranged from +0.12 to +0.34 ‰, with an average of +0.26 ± 0.04 ‰ (2 s) for sediments (N = 6), +0.23 ± 0.05 ‰ (2 s) for SPM (N = 6), +0.30 ± 0.04 ‰ (2 s) for soil (N = 1), and +0.30 ± 0.01 ‰ (2 s) for rock (N = 1), where "N" is the number of samples. The lowest $\delta^{66/64}Zn_{JMC}$ value of +0.12 ± 0.02 ‰ (n = 4, 2 s) and the highest $\delta^{66/64}Zn_{JMC}$ value of +0.34 ± 0.02 ‰ (n = 2, 2 s) correspond to the SPM sample and surficial sediment samples from the R3 site, respectively.

3 Discussion

3.1 Metal pollution status of the PSR-GR fluvial basin

Our results of dissolved Cd, Cr, Cu, and Pb are at least five times smaller than the reported on a previous study in the PSR-GR basin (**Table 1**) conducted in the same wet season (Pfeiffer et al., 1986). Zinc concentrations remain close to those found in this previous study. Concentrations of all dissolved metals do not exceed the WHO standard and the USEPA recommendations and the dissolved phase from PSR-GR were considerably less polluted than that reported in the other anthropized rivers (densely populated and industrialized) in China (Liu et al., 2018).

The values of SPM concentrations reported in the PSR-GR basin were in the same range as those obtained in the previous study (**Table 1**, $p > 0.05$) of Pfeiffer et al. (1986) and relatively lower than those the anthropized Zhujiang River, southwest China (Zeng et al., 2019). All average concentrations of metals in sediments were higher than the R3-soil and the non-contaminated sediment R0 (**Table S9**), sampled upstream the PSR (see **Fig. 1** in the lower right rectangle).

According to Chen et al. (2007), the mean EF values obtained for surficial sediments in this study were described as moderate to enriched for As, Cr, and Zn, slightly enriched for Cd and Hg, and not enriched for Cu and Pb (**Fig. S2a**). The sum of EF (∑EF) values of trace metals,

displayed in **Table S9**, can indicate the pollution degree in the following order: R1 > R3 > R4 > R6 > R2 > R5. The current status of trace metals contamination (Cd, Cr, Cu, Pb, and Zn) in sediments is presented with an insignificant difference (t-test, $p > 0.05$) compared to a previous study in the same area (Pfeiffer et al., 1986). The total Hg average concentration in sediments (262 ± 86.3 ng/g) was similar to previous studies from PSR-GR system (Marins et al., 1998; Molisani et al., 2004) and shows an enrichment by a factor of 3 if compared to the local background of 86 ng/g (Gonçalves et al., 2018).

The metals concentrations in PSR-GR sediments were higher than those reported in the Jinjiang River (**Table 1**), a Chinese anthropized river (Liu et al., 2018), reaching values two times higher for Cr and Zn. Differently, the PSR-GR sediments revealed Cd, Cr, Cu, Pb, and Zn concentrations almost two-fold below than those of the Tietê-Pinheiros River located in the most industrialized and populated megacity of Brazil (da Silva et al., 2002).

3.2 **Identifying natural and anthropogenic sources by multivariate analysis**

The cluster of R1 and R2 sites in the PCA of the dissolved phase (**Fig. 2b**) can be related to diffuse sources from sewage and agriculture runoff (Macintosh et al., 2018). The R6 site was correlated with dissolved Cr and Zn, indicating industrial sources, as well as suggested by Molisani et al. (2006).

The PC1 of SPM data set grouped trace metals with POC and associated these variables with R1, R2, and R4 sites. The map of **Fig. 1** shows that the R1 and R2 sites are located downstream from a colossal steel industrial park (SCN), while the R4 site is located in a dense traffic area, nearby an industrial park (Queimados, Rio de Janeiro), and immediately downstream of two gas-fired power plants (thermoelectric). These activities can be noteworthy pollution sources of trace metals (Ćujić et al., 2016; Huber et al., 2016; Sethurajan et al., 2016). High Cd concentrations in the SPM of the R6 site evidenced a punctual well-known urban pollution (Le Gall et al., 2018). The multivariate statistics of the SPM phase showed that R3 and R5 sites are the least polluted ones.

The X-ray diffractograms showed important secondary minerals in the SPM phase, such as gibbsite and clay minerals (kaolinite and muscovite) (**Fig. S1a**). The transport of trace metals in fluvial systems is expected to take place while they're sorbed to sediment particles (Sutherland, 2000). The Fe and Al oxyhydroxides, including a coating on mineral surfaces,

constitute the main bearing phases to effectively sorb trace metals, as appointed by Brown and Calas (2011). All the results in this study point out the key role of the SPM phase in the behavior and transport of trace metals in the studied rivers. Moreover, the lack of linear trend of metal concentrations in the downstream direction is likely provoked by favorable decantation of SPM particles metal-enriched at lentic/lotic interface in the reservoirs just upstream the R3 and R5 sites (Molisani et al., 2006). Beyond that, increases in concentrations downstream for some elements, such as Cd and Zn, were induced by additional inputs of anthropogenic sources.

The PCA results of the surface sediments (**Fig. 2f**) suggested that the lithogenic sources predominate in the R3 site, while urban effluent indicators, such as P, correlate with R2 and R1 sites. Phosphorus origins could be related to multiple sources in the watershed, such as agricultural and sewage residues (Rodrigues et al., 2013). Furthermore, this PCA suggested that the R1 site was polluted by As sources, while the R4 site was polluted by Pb and Zn sources.

3.3 Geochemical partitioning of trace metals

The higher percentages of metals found in the residual fraction (F4) were 79%, 78%, 80%, and 47%, for As, Cd, Cr, and Cu, respectively, which indicates that a considerable part of these metals is originated from the lithogenic sources (Davila et al., 2020). We hypothesize that the weathering of mafic-orthogranulites rocks from the Paraiba do Sul and Juiz de Fora domains (Heilbron and Machado, 2003; Kuribara et al., 2019) can contribute to the slight metals enrichment appointed in sediments.

The Zn concentrations in the exchangeable/carbonate fraction presented a significant contribution (ZnF1 average of 29%), while the other metals reached a maximum of 9%. As also suggested by metal concentrations in SPM and sediments (**Fig. 2c and Fig. 2e**), Zn is identified as the main metal contaminant and displayed higher mobility and ecological risk. A high concentration of exchangeable/carbonate Zn, mainly in the R1 and R4 sites, argues for a higher potentially bioavailable pool that may affect water quality and biota (Rosado et al., 2016). These results are in line with recent findings on GR, which pointed out the high concentration of Zn in aquatic macrophytes correlated with a high concentration in SPM (Valitutto et al., 2007), and another study that shows a high Zn bioaccumulation in fish gonads in the PSR (Calza et al., 2004).

The elevated percentual values of the reducible fraction of Pb and Zn (53 and 19% on average, respectively), compared with other metals (ranging from 5 and 18%), suggest that these elements can be remobilized through the reduction and dissolution of Fe and Mn oxyhydroxides during anoxic events in post-depositional processes (Rigaud et al., 2013). Such a mechanism that leads to metal release is known to occur in the sediments of lentic ecosystems (Gao et al., 2018) and represents a potential environmental risk. In distinction to Pb and Zn, the F3 fraction was the second fraction more important for Cr and Cu (14 and 26%, on average, respectively), showing the high affinity of these metals to organic matter and sulfides ligands (Charriau et al., 2011).

3.4 Investigating Zn sources and mixing processes using Zn isotopes

The Zn isotopic data plotted against the ratio Zn/Al displays a well-correlated inverse trend ($r^2 > 0.80$, dotted lines, $p < 0.05$; **Fig. 3**). These results are consistent with the occurrence of two dominant endmembers often reported in the literature: one lithogenic/background $\delta^{66/64}Zn_{JMC} \approx +0.30$ ‰ (light blue area, **Fig. 3**) (e.g., Chen et al., 2013), and the other, anthropogenic $\delta^{66/64}Zn_{JMC} \approx +0.15$ ‰ (light red area, **Fig. 3**) (John et al., 2007). The variation in the $\delta^{66/64}Zn_{JMC}$ values along the studied rivers seems to be related to many anthropogenic inputs or scavenging outputs.

The main lithogenic sources derived from weathered material coming from rocks and soils have an isotopic composition of $\delta^{66/64}Zn_{JMC}$ of +0.30 ‰, which is an average of $\delta^{66/64}Zn_{JMC}$ values for reference materials (granite G-2 = +0.34 ± 0.04 ‰, 2 s, and granodiorite GSP-1 = +0.31 ± 0.05 ‰, 2 s, Chen et al., 2016), Upper Continental Crust, UCC (+0.28 ± 0.05 ‰, 2 s, Chen et al., 2013), and local terrestrial background previously studied in Sepetiba Bay (+0.28 ± 0.12‰, 2 s, n = 3, Araújo et al., 2017a). This lithogenic signature is similar to Zn isotope composition of granite rock R6 ($\delta^{66/64}Zn_{JMC}$ = +0.30 ‰ ± 0.01, n = 2, 2 s, **Table 2**). Likewise, the $\delta^{66/64}Zn_{JMC}$ values in sediments and SPM of the least contaminated site (R5) match the lithogenic isotope composition. These considerations along with the Zn partition in this site, mainly associated with the residual fraction (ZnF4 = 57%), suggest that the sediments and SPM of the R5 site were dominated by lithogenic sources.

The lightest $\delta^{66/64}Zn_{JMC}$ signature of SPM at the R3 site seems to be an outlier (**Fig. 3**) since the multivariate statistical analysis shows a weak correlation with pollution (**Fig. 2d**). Previously, shifts towards light isotope compositions in the SPM have been associated with the

biological uptake from the primary activity of an unpolluted Swiss lake (Peel et al., 2009). The authors argued that the preferential uptake of lighter Zn isotopes yields, at the end of the productive period, algae debris enriched with the light isotope and may contribute to a final isotope budget in the particulate phase lighter than the lithogenic isotope signature. Thus, the light Zn signature of the R3 site can be related to a Zn-bearing organic pool originated from the algal bloom in the upstream reservoirs from the R3 site (Vigario and Ponte Coberta, **Fig. 1**). Overall, the $\delta^{66/64}Zn_{JMC}$ signature of SPM at the R3 site may represent the sum of the signatures from the lithogenic source by weathering, the anthropogenic source inserted upstream, and potential additional fractionation provoked by biological uptake processes.

As pointed out by previous studies, steel, metallurgical, and chemical plants, power production, heavy road traffic, and urban runoff are expected to be the main sources of Zn contamination in the PSR-GR watershed (Sullivan and Worsley, 2002). All these anthropogenic activities may introduce light $\delta^{66/64}Zn_{JMC}$ signatures (Yin et al., 2015), summarized in the light red rectangle of **Fig. 3**. As an example of the Zn input by these sources, the high temperature employed in coal-fired power plants and pyrometallurgy industries is known for fractionating the Zn isotopes in the feed material (coal and ores, respectively), leading to enrichment of lighter isotopes into the atmospheric exhausts (Gonzalez et al., 2016; Yin et al., 2015). This fractionation process can be modeled using the Rayleigh-type fractionation following a unidirectional fractionation (for more details see Wiederhold, 2015). Even though not all sources have been specifically characterized in the literature, the overall average light signatures of $+0.15 \pm 0.05$ ‰ from these anthropogenic pollution sources (a light red rectangle of **Fig. 3**) were compatible with the anthropogenic endmembers suggested by (Desaulty and Petelet-Giraud, 2020). The multivariate statistics discussed in previous sections and the higher percentages of Zn in the more available fractions (F1+F1+F3 = 86%), lead us to suggest that the sediment and SPM of the R4 site are dominated by anthropogenic sources, with the $\delta^{66/64}Zn_{JMC}$ in agreement with the isotope fingerprints attributed to those.

The surficial sediments at R1, R2, R3, and R6 presented a $\delta^{66/64}Zn_{JMC}$ comparable to lithogenic Zn isotope signature, despite these sediments being relatively richer in total Zn (ranging from 164 to 173 $\mu g\ g^{-1}$). As discussed earlier, there is an encompassing of sources in some industrialized areas of the PSR-GR basin. Thus, the lack of a significant $\delta^{66/64}Zn_{JMC}$ shift leads us to suppose that the mixing processes of lithogenic and anthropogenic Zn are dominated by the former in these sites.

The scheme in **Fig. 4** summarizes the main metal inputs and outputs in the dissolved and suspended phases, including the main water reservoirs, the potential sources of pollution, as interpreted from our geochemical approaches, and the expected metal removal from the water column by sedimentation along the studied rivers. Though a precise quantification of specific anthropogenic contributions is a difficult task for the relatively narrow ranges of $\delta^{66/64}Zn_{JMC}$ signatures observed, as also reported for other rivers and estuaries (Tu et al., 2020; Zimmermann et al., 2020), the lighter anthropogenic $\delta^{66/64}Zn_{JMC}$ is coherent with the sum of more mobile fractions of Zn (F1, F2, and F3) in polluted sites. The results are indicative of a conservative mixing source between the two endmembers. Also, experimental data were consistent with previous studies that found Zn isotopes compositions predominantly controlled by a binary mixing between a lithogenic material ($\delta^{66/64}Zn_{JMC} \approx +0.30$ ‰) and Zn issued from multiple anthropogenic sources, which yield an average $\delta^{66/64}Zn_{JMC} \approx +0.10$ ‰ (Araújo et al., 2019; Chen et al., 2009a; Thapalia et al., 2015). Therefore, the combination of the multiple geochemical tools used here allowed the identification of anthropogenic influences along the waterways studied, as summarized in **Fig. 4**.

4 Conclusions

Our integrated approach of stable Zn isotopes, selective sequential extractions (BCR), and multivariate statistics (PCA) was helpful to the source assessment and to elucidate the mixing process of these sources in the complex Paraíba do Sul and Guandu Rivers diversion system, Brazil. In sediments, the elements As, Cr, and Cu presented low enrichment factors and preferential association with the residual fraction (F4), implying low potential availability and predominance of lithogenic sources. Zinc and Pb showed high enrichment factors and significant percentual levels in exchangeable/carbonate (F1) and reducible (F2) fractions, indicating higher mobility and predominance of anthropogenic sources. Our results also indicated that Fe and Al oxyhydroxides play a key role in the mechanism of trace metal transport in the studied rivers, particularly for Zn. An inverse correlation between $\delta^{66/64}Zn$ and Zn/Al ratio suggests a mixing source process involving lithogenic and anthropogenic endmembers.

Furthermore, the sum of labile fractions of Zn (F1, F2, and F3) in the polluted site was consistent with the lighter anthropogenic $\delta^{66/64}Zn_{JMC}$ signature and the high percentages of Zn in the residual fraction (F4) was observed in the less contaminated site with lithogenic $\delta^{66/64}Zn_{JMC}$. However, as reported for other rivers and estuaries (Tu et al., 2020; Zimmermann

et al., 2020), precise quantification of specific industrial and urban anthropogenic contributions is a difficult task due to the relatively narrow $\delta^{66/64}Zn_{JMC}$ signatures among these sources and the lithogenic one. Some of these drawbacks can be overcome by integrating multi-geochemical tools, mainly in watersheds with a history of pollution associated with diffuse emissions by metal sources. The "tool-box" proposed in this study, coupling stable Zn isotopes, selective sequential extractions (BCR), and multivariate statistics (PCA), may be suitable to study complex aquatic systems worldwide.

Acknowledgments

This study was financed in part by the Coordenação de Aperfeiçoamento de Pessoal de Nível Superior - Brasil (CAPES) - Finance Code 001. God bless us. The authors acknowledge the students and researchers who participated in field investigations. The authors acknowledge the staff from the Geosciences Institute of UnB, and Hydrosciences Montpellier, particularly Dr. Remi Freydier, Bárbara Alcântara Lima, Jeane Grasielly, and the PPGG and PPGGAG. Analytical work in Brazil and France was partly funded by the LMI-OCE and CNPq 400029/2015-4, 420697/2018-7. Jeremie Garnier was supported by CNPq grant 302722/2018-1. We acknowledge to symbols courtesy of the Integration and Application Network (ian.umces.edu/symbols/).

Appendix A. Supplementary data

Supplementary data associated with this article can be found in the online version.

References

Araújo, D.F., Boaventura, G.R., Machado, W., Viers, J., Weiss, D., Patchineelam, S.R., Ruiz, I., Rodrigues, A.P.C., Babinski, M., Dantas, E., 2017a. Tracing of anthropogenic zinc sources in coastal environments using stable isotope composition. Chem. Geol. 449, 226–235. https://doi.org/10.1016/j.chemgeo.2016.12.004

Araújo, D.F., Boaventura, G.R., Viers, J., Mulholland, D.S., Weiss, D., Araújo, D., Lima, B., Ruiz, I., Machado, W., Babinski, M., Dantas, E., 2017b. Ion exchange chromatography and mass bias correction for accurate and precise Zn isotope ratio measurements in

environmental reference materials by MC-ICP-MS. J. Braz. Chem. Soc. 28, 225–235. https://doi.org/10.5935/0103-5053.20160167

Araújo, D.F., Ponzevera, E., Briant, N., Knoery, J., Sireau, T., Mojtahid, M., Metzger, E., Brach-Papa, C., 2019. Assessment of the metal contamination evolution in the Loire estuary using Cu and Zn stable isotopes and geochemical data in sediments. Mar. Pollut. Bull. 143, 12–23. https://doi.org/10.1016/j.marpolbul.2019.04.034

Barcellos, C., Lacerda, L.D., 1994. Cadmium and zinc source assessment in the Sepetiba Bay and basin region. Environ. Monit. Assess. 29, 183–199. https://doi.org/10.1007/BF00546874

Britto, A.L., Johnsson, R.M.F., Carneiro, P.R.F., 2016. Water supply and hydrosocial scarcity in the rio de janeiro metropolitan area1. Ambient. e Soc. 19, 183–206. https://doi.org/10.1590/1809-4422ASOC150159R1V1912016

Brown, G.E., Calas, G., 2011. Minéralogie environnementale: comprendre le comportement des éléments dans les écosystèmes. Comptes Rendus - Geosci. 343, 90–112. https://doi.org/10.1016/j.crte.2010.12.005

Calza, C., Anjos, M.J., Castro, C.R.F., Barroso, R.C., Araujo, F.G., Lopes, R.T., 2004. Evaluation of heavy metals levels in the Paraíba do Sul River by SRTXRF in muscle, gonads and gills of Geophagus brasiliensis. Radiat. Phys. Chem. 71, 787–788. https://doi.org/10.1016/j.radphyschem.2004.04.092

Charriau, A., Lesven, L., Gao, Y., Leermakers, M., Baeyens, W., Ouddane, B., Billon, G., 2011. Trace metal behaviour in riverine sediments: Role of organic matter and sulfides. Appl. Geochemistry 26, 80–90. https://doi.org/10.1016/j.apgeochem.2010.11.005

Chen, J. Bin, Gaillardet, J., Louvat, P., Huon, S., 2009a. Zn isotopes in the suspended load of the Seine River, France: Isotopic variations and source determination. Geochim. Cosmochim. Acta 73, 4060–4076. https://doi.org/10.1016/j.gca.2009.04.017

Chen, J. Bin, Louvat, P., Gaillardet, J., Birck, J.L., 2009b. Direct separation of Zn from dilute aqueous solutions for isotope composition determination using multi-collector ICP-MS. Chem. Geol. 259, 120–130. https://doi.org/10.1016/j.chemgeo.2008.10.040

Chen, C.W., Kao, C.M., Chen, C.F., Dong, C. Di, 2007. Distribution and accumulation of heavy metals in the sediments of Kaohsiung Harbor, Taiwan. Chemosphere 66, 1431–

1440. https://doi.org/10.1016/j.chemosphere.2006.09.030

Chen, H., Savage, P.S., Teng, F.Z., Helz, R.T., Moynier, F., 2013a. Zinc isotope fractionation during magmatic differentiation and the isotopic composition of the bulk Earth. Earth Planet. Sci. Lett. 369–370, 34–42. https://doi.org/10.1016/j.epsl.2013.02.037

Chen, S., Liu, Y., Hu, J., Zhang, Z., Hou, Z., Huang, F., Yu, H., 2016. Zinc Isotopic Compositions of NIST SRM 683 and Whole-Rock Reference Materials. Geostand. Geoanalytical Res. 40, 417–432. https://doi.org/10.1111/j.1751-908X.2015.00377.x

CPRM – Serviço Geológico do Brasil, 2000. Dignóstico Geoambiental do Estado do Rio de Janeiro CD-ROM.

Ćujić, M., Dragović, S., Dordević, M., Dragović, R., Gajić, B., 2016. Environmental assessment of heavy metals around the largest coal fired power plant in Serbia. Catena 139, 44–52. https://doi.org/10.1016/j.catena.2015.12.001

da Silva, I.S., Abate, G., Lichtig, J., Masini, J.C., 2002. Heavy metal distribution in recent sediments of the Tietê -Pinheiros river system in São Paulo state , Brazil. Appl. Geochemistry 17, 105–116. https://doi.org/10.1016/S0883-2927(01)00086-5

Davila, R.B., Fontes, M.P.F., Pacheco, A.A., Ferreira, M. da S., 2020. Heavy metals in iron ore tailings and floodplain soils affected by the Samarco dam collapse in Brazil. Sci. Total Environ. 709. https://doi.org/10.1016/j.scitotenv.2019.136151

Desaulty, A.-M., Petelet-Giraud, E., 2020. Zinc isotope composition as a tool for tracing sources and fate of metal contaminants in rivers. Sci. Total Environ. 138599. https://doi.org/https://doi.org/10.1016/j.scitotenv.2020.138599

Dong, S., Ochoa Gonzalez, R., Harrison, R.M., Green, D., North, R., Fowler, G., Weiss, D., 2017. Isotopic signatures suggest important contributions from recycled gasoline, road dust and non-exhaust traffic sources for copper, zinc and lead in PM10 in London, United Kingdom. Atmos. Environ. 165, 88–98. https://doi.org/10.1016/j.atmosenv.2017.06.020

Du Laing, G., Rinklebe, J., Vandecasteele, B., Meers, E., Tack, F.M.G., 2009. Trace metal behaviour in estuarine and riverine floodplain soils and sediments: A review. Sci. Total Environ. 407, 3972–3985. https://doi.org/10.1016/j.scitotenv.2008.07.025

Gao, L., Wang, Z., Li, S., Chen, J., 2018. Chemosphere Bioavailability and toxicity of trace

591 metals (Cd , Cr , Cu , Ni , and Zn) in sediment cores from the Shima River , South
592 China. Chemosphere 192, 31–42. https://doi.org/10.1016/j.chemosphere.2017.10.110

593 Gonçalves, R.A., Oliveira, D.F., Ferreira, P.H.G., Rezende, C.E., Almeida, P., de Lacerda,
594 L.D., Godoy, J.M., 2018. Decadal and spatial variation of Hg concentrations in
595 sediments of a multi-stressor impacted estuary. Mar. Pollut. Bull. 135, 1158–1163.
596 https://doi.org/10.1016/j.marpolbul.2018.08.053

597 Gonzalez, R.O., Strekopytov, S., Amato, F., Querol, X., Reche, C., Weiss, D., 2016. New
598 Insights from Zinc and Copper Isotopic Compositions into the Sources of Atmospheric
599 Particulate Matter from Two Major European Cities. Environ. Sci. Technol. 50, 9816–
600 9824. https://doi.org/10.1021/acs.est.6b00863

601 Hahn, J., Opp, C., Evgrafova, A., Groll, M., Zitzer, N., Laufenberg, G., 2018. Impacts of dam
602 draining on the mobility of heavy metals and arsenic in water and basin bottom
603 sediments of three studied dams in Germany. Sci. Total Environ. 640–641, 1072–1081.
604 https://doi.org/10.1016/j.scitotenv.2018.05.295

605 Heilbron, M., Machado, N., 2003. Timing of terrane accretion in the Neoproterozoic –
606 Eopaleozoic Ribeira orogen (se Brazil) 125, 87–112. https://doi.org/10.1016/S0301-
607 9268(03)00082-2

608 Huber, M., Welker, A., Helmreich, B., 2016. Critical review of heavy metal pollution of
609 traffic area runoff: Occurrence, influencing factors, and partitioning. Sci. Total Environ.
610 541, 895–919. https://doi.org/10.1016/j.scitotenv.2015.09.033

611 IUSS Working Group WRB, 2014. World reference base for soil resources 2014.
612 International soil classification system for naming soils and creating legends for soil
613 maps, World Soil Resources Reports No. 106.
614 https://doi.org/10.1017/S0014479706394902

615 John, S.G., Genevieve Park, J., Zhang, Z., Boyle, E.A., 2007. The isotopic composition of
616 some common forms of anthropogenic zinc. Chem. Geol. 245, 61–69.
617 https://doi.org/10.1016/j.chemgeo.2007.07.024

618 Kuribara, Y., Tsunogae, T., Santosh, M., Takamura, Y., Costa, A.G., Rosière, C.A., 2019.
619 Eoarchean to Neoproterozoic crustal evolution of the Mantiqueira and the Juiz de Fora
620 Complexes, SE Brazil: Petrology, geochemistry, zircon U-Pb geochronology and Lu-Hf
621 isotopes. Precambrian Res. 323, 82–101.

https://doi.org/10.1016/j.precamres.2019.01.008

Le Gall, M., Ayrault, S., Evrard, O., Laceby, J.P., Gateuille, D., Lefèvre, I., Mouchel, J.M., Meybeck, M., 2018. Investigating the metal contamination of sediment transported by the 2016 Seine River flood (Paris, France). Environ. Pollut. 240, 125–139. https://doi.org/10.1016/j.envpol.2018.04.082

Li, Wei, Gou, W., Li, Weiqiang, Zhang, T., Yu, B., Liu, Q., Shi, J., 2019. Environmental applications of metal stable isotopes: Silver, mercury and zinc. Environ. Pollut. 252, 1344–1356. https://doi.org/10.1016/j.envpol.2019.06.037

Liu, X., Jiang, J., Yan, Y., Dai, Y.Y., Deng, B., Ding, S., Su, S., Sun, W., Li, Z., Gan, Z., 2018. Distribution and risk assessment of metals in water, sediments, and wild fish from Jinjiang River in Chengdu, China. Chemosphere 196, 45–52. https://doi.org/10.1016/j.chemosphere.2017.12.135

Macintosh, K.A., Mayer, B.K., McDowell, R.W., Powers, S.M., Baker, L.A., Boyer, T.H., Rittmann, B.E., 2018. Managing Diffuse Phosphorus at the Source versus at the Sink. Environ. Sci. Technol. 52, 11995–12009. https://doi.org/10.1021/acs.est.8b01143

Mäkelä, M., Heikinheimo, E., Välimäki, I., Dahl, O., 2015. Characterization of industrial secondary desulphurization slag by chemical fractionation with supportive X-ray diffraction and scanning electron microscopy. Int. J. Miner. Process. 134, 29–35. https://doi.org/https://doi.org/10.1016/j.minpro.2014.11.006

Maréchal, C.N., Télouk, P., Albarède, F., 1999. Precise analysis of copper and zinc isotopic compositions by plasma-source mass spectrometry. Chem. Geol. 156, 251–273. https://doi.org/10.1016/S0009-2541(98)00191-0

Marins, R. V., Lacerda, L.D., Paraquetti, E.C.P., Vilas Boas, R.C., 1998. Geochemistry of Mercury in sepetiba bay, Southeastern Brazil. Bull. Environ. Contam. Toxicol. 61, 57–64.

Marins, R. V., Machado, W., Paraquetti, H.H.M., Bidone, E.D., Lacerda, L.D., Molisani, M.M., 2004. Environmental changes in Sepetiba Bay, SE Brazil. Reg. Environ. Chang. 4, 17–27. https://doi.org/10.1007/s10113-003-0060-9

Marques, E.D., Tubbs, D., Gomes, O.V.O., Silva-Filho, E. V., 2012. Influence of acid sand pit lakes in surrounding groundwater chemistry, Sepetiba sedimentary basin, Rio de

652 Janeiro, Brazil. J. Geochemical Explor. 112, 306–321.
653 https://doi.org/10.1016/j.gexplo.2011.10.002

654 Miguens, F.C., de Oliveira, M.L., Ferreira, A. de O., Barbosa, L.R., Melo, E.J.T. de, de
655 Carvalho, C.E.V., 2016. Structural and elemental analysis of bottom sediments from the
656 Paraíba do Sul River (SE, Brazil) by analytical microscopy. J. South Am. Earth Sci. 66,
657 82–96. https://doi.org/10.1016/j.jsames.2015.12.009

658 Molisani, M.M., Kjerfve, B., Barreto, R., Drude de Lacerda, L., 2007. Land-sea mercury
659 transport through a modified watershed, SE Brazil. Water Res. 41, 1929–1938.
660 https://doi.org/10.1016/j.watres.2007.02.007

661 Molisani, M.M., Kjerfve, B., Silva, A.P., Lacerda, L.D., 2006a. Water discharge and sediment
662 load to Sepetiba Bay from an anthropogenically-altered drainage basin, SE Brazil. J.
663 Hydrol. 331, 425–433. https://doi.org/10.1016/j.jhydrol.2006.05.038

664 Molisani, M.M., Marins, R. V., Machado, W., Paraquetti, H.H.M., Bidone, E.D., Lacerda,
665 L.D., 2004. Environmental changes in Sepetiba Bay, SE Brazil. Reg. Environ. Chang. 4,
666 17–27. https://doi.org/10.1007/s10113-003-0060-9

667 Molisani, M.M., Rocha, R., Machado, W., Barreto, R.C., Lacerda, L.D., 2006e. Mercury
668 contents in aquatic macrophytes from two reservoirs in the Paraíba do Sul: Guandú river
669 system, SE Brazil. Brazilian J. Biol. 66, 101–107. https://doi.org/10.1590/S1519-
670 69842006000100013

671 Moynier, F., Vance, D., Fujii, T., Savage, P., 2017. The Isotope Geochemistry of Zinc and
672 Copper. Rev. Mineral. Geochemistry 82, 543–600.
673 https://doi.org/10.2138/rmg.2017.82.13

674 Peel, K., Weiss, D., Sigg, L., 2009. Zinc isotope composition of settling particles as a proxy
675 for biogeochemical processes in lakes: Insights from the eutrophic Lake Greifen,
676 Switzerland. Limnol. Oceanogr. 54, 1699–1708.
677 https://doi.org/10.4319/lo.2009.54.5.1699

678 Petit, J.C.J., Schäfer, J., Coynel, A., Blanc, G., Chiffoleau, J.F., Auger, D., Bossy, C.,
679 Derriennic, H., Mikolaczyk, M., Dutruch, L., Mattielli, N., 2015. The estuarine
680 geochemical reactivity of Zn isotopes and its relevance for the biomonitoring of
681 anthropogenic Zn and Cd contaminations from metallurgical activities: Example of the
682 Gironde fluvial-estuarine system, France. Geochim. Cosmochim. Acta 170, 108–125.

https://doi.org/10.1016/j.gca.2015.08.004

Pfeiffer, W.C., Fiszman, M., Malm, O., Maurício Azcue, J., 1986. Heavy metal pollution in the Paraiba do sul River, Brazil. Sci. Total Environ. 58, 73–79. https://doi.org/https://doi.org/10.1016/0048-9697(86)90077-X

Rauret, G., López-Sánchez, J.-F., Sahuquillo, A., Barahona, E., Lachica, M., Ure, A.M., Davidson, C.M., Gomez, A., Lück, D., Bacon, J., Yli-Halla, M., Muntau, H., Quevauviller, P., 2000. Application of a modified BCR sequential extraction (three-step) procedure for the determination of extractable trace metal contents in a sewage sludge amended soil reference material (CRM 483), complemented by a three-year stability study of acetic acid . J. Environ. Monit. 2, 228–233. https://doi.org/10.1039/b001496f

Resongles, E., Casiot, C., Freydier, R., Dezileau, L., Viers, J.Ô., Elbaz-Poulichet, F., 2014. Persisting impact of historical mining activity to metal (Pb, Zn, Cd, Tl, Hg) and metalloid (As, Sb) enrichment in sediments of the Gardon River, Southern France. Sci. Total Environ. 481, 509–521. https://doi.org/10.1016/j.scitotenv.2014.02.078

Rigaud, S., Radakovitch, O., Couture, R.M., Deflandre, B., Cossa, D., Garnier, C., Garnier, J.M., 2013. Mobility and fluxes of trace elements and nutrients at the sediment-water interface of a lagoon under contrasting water column oxygenation conditions. Appl. Geochemistry 31, 35–51. https://doi.org/10.1016/j.apgeochem.2012.12.003

Rodrigues, S.K., Abessa, D.M.S., Machado, E.C., 2013. Geochemical and ecotoxicological assessment for estuarine surface sediments from Southern Brazil. Mar. Environ. Res. 91, 68–79. https://doi.org/10.1016/j.marenvres.2013.02.005

Rosado, D., Usero, J., Morillo, J., 2016. Assessment of heavy metals bioavailability and toxicity toward Vibrio fischeri in sediment of the Huelva estuary. Chemosphere 153, 10–17. https://doi.org/10.1016/j.chemosphere.2016.03.040

Santos-Neves, J.M., Marques, E.D., Kütter, V.T., Lacerda, L.D. de, Sanders, C.J., Sella, S.M., Silva-Filho, E.V., 2018. Influence of River Water Diversion on Hydrogeochemistry and Ree Distribution, Rio De Janeiro, Brazil. Carpathian J. earth Environ. Sci. 13, 453–464. https://doi.org/10.26471/cjees/2018/013/039

Santos-Neves, J.M., Marques, E.D., Kütter, V.T., Lacerda, L.D., Sanders, C.J., Sella, S.M., Silva-FILHO, E.V., 2018. Influence of River Water Diversion on Hydrogeochemistry and Ree Distribution, Rio De Janeiro, Brazil. Carpathian J. Earth Environ. Sci. 13, 453–

464. https://doi.org/10.26471/cjees/2018/013/039

Sethurajan, M., Huguenot, D., Lens, P.N.L., Horn, H.A., 2016. Fractionation and leachability of heavy metals from aged and recent Zn metallurgical leach residues from the Três Marias zinc plant (Minas Gerais , Brazil). Environ. Sci. Pollut. Res. https://doi.org/10.1007/s11356-015-6014-1

Souto-Oliveira, C.E., Babinski, M., Araújo, D.F., Weiss, D.J., Ruiz, I.R., 2019. Multi-isotope approach of Pb, Cu and Zn in urban aerosols and anthropogenic sources improves tracing of the atmospheric pollutant sources in megacities. Atmos. Environ. 198, 427–437. https://doi.org/10.1016/j.atmosenv.2018.11.007

Sullivan, J.H., Worsley, D.A., 2002. Zinc runoff from galvanised steel materials exposed in industrial/marine environment. Br. Corros. J. 37, 282–288. https://doi.org/10.1179/000705902225006697

Sutherland, Ross A., 2000. A comparison of geochemical information obtained from two fluvial bed sediment fractions. Environ. Geol. 39, 330–341. https://doi.org/10.1007/s002540050012

Sutherland, R. A., 2000. Bed sediment-associated trace metals in an urban stream, Oahu, Hawaii. Environ. Geol. 39, 611–627. https://doi.org/10.1007/s002540050473

Thapalia, A., Borrok, D.M., Van Metre, P.C., Musgrove, M., Landa, E.R., 2010. Zn and Cu isotopes as tracers of anthropogenic contamination in a sediment core from an Urban Lake. Environ. Sci. Technol. 44, 1544–1550. https://doi.org/10.1021/es902933y

Thapalia, A., Borrok, D.M., Van Metre, P.C., Wilson, J., 2015. Zinc isotopic signatures in eight lake sediment cores from across the United States. Environ. Sci. Technol. 49, 132–40. https://doi.org/10.1021/es5036893

Tonhá, M.S., Garnier, J., Araújo, D.F., Cunha, B.C.A., Machado, W., Dantas, E., Araújo, R., Kutter, V.T., Bonnet, M., Seyler, P., 2020. Science of the Total Environment Behavior of metallurgical zinc contamination in coastal environments : A survey of Zn from electroplating wastes and partitioning in sediments. Sci. Total Environ. 743, 140610. https://doi.org/10.1016/j.scitotenv.2020.140610

Tu, Y., You, C., Kuo, T., 2020. Chemosphere Source identi fi cation of Zn in Erren River , Taiwan : An application of Zn isotopes. Chemosphere 248, 126044.

744 https://doi.org/10.1016/j.chemosphere.2020.126044

745 USEPA, 2000. National Recommended Water Quality Criteria. Appl. Environ. Chem.
746 https://doi.org/10.1201/9781420032963.axb

747 Valitutto, R.S., Sella, S.M., Silva-Filho, E. V., Pereira, R.G., Miekeley, N., 2007a.
748 Accumulation of metals in macrophytes from water reservoirs of a power supply plant,
749 Rio de Janeiro State, Brazil. Water. Air. Soil Pollut. 178, 89–102.
750 https://doi.org/10.1007/s11270-006-9154-6

751 WHO, 2017. Guidelines for drinking-water quality. World Health Organization.

752 Wiederhold, J.G., 2015. Metal stable isotope signatures as tracers in environmental
753 geochemistry. Environ. Sci. Technol. 49, 2606–2624. https://doi.org/10.1021/es504683e

754 Xia, Y., Gao, T., Liu, Y., Wang, Z., Liu, C., Wu, Q., Qi, M., Lv, Y., Li, F., 2020. Zinc isotope
755 revealing zinc's sources and transport processes in karst region. Sci. Total Environ. 724,
756 138191. https://doi.org/10.1016/j.scitotenv.2020.138191

757 Yin, N.H., Sivry, Y., Benedetti, M.F., Lens, P.N.L., van Hullebusch, E.D., 2015. Application
758 of Zn isotopes in environmental impact assessment of Zn-Pb metallurgical industries: A
759 mini review. Appl. Geochemistry 64, 128–135.
760 https://doi.org/10.1016/j.apgeochem.2015.09.016

761 Zeng, J., Han, G., Wu, Q., Tang, Y., 2019. Heavy metals in suspended particulate matter of
762 the Zhujiang River, southwest China: Contents, sources, and health risks. Int. J. Environ.
763 Res. Public Health 16. https://doi.org/10.3390/ijerph16101843

764 Zhang, C., Yu, Z. gang, Zeng, G. ming, Jiang, M., Yang, Z. zhu, Cui, F., Zhu, M. ying, Shen,
765 L. qing, Hu, L., 2014. Effects of sediment geochemical properties on heavy metal
766 bioavailability. Environ. Int. 73, 270–281. https://doi.org/10.1016/j.envint.2014.08.010

767 Zhao, X., Yao, L., Ma, Q., Zhou, G., Wang, L., Fang, Q., 2018. Chemosphere Distribution
768 and ecological risk assessment of cadmium in water and sediment in Longjiang River ,
769 China : Implication on water quality management after pollution accident. Chemosphere
770 194, 107–116. https://doi.org/10.1016/j.chemosphere.2017.11.127

771 Zimmermann, T., Mohamed, A.F., Reese, A., Wieser, M.E., Kleeberg, U., Pröfrock, D.,
772 Irrgeher, J., 2020. Zinc isotopic variation of water and surface sediments from the
773 German Elbe River. Sci. Total Environ. 707, 1–10.

https://doi.org/10.1016/j.scitotenv.2019.135219

List of figures

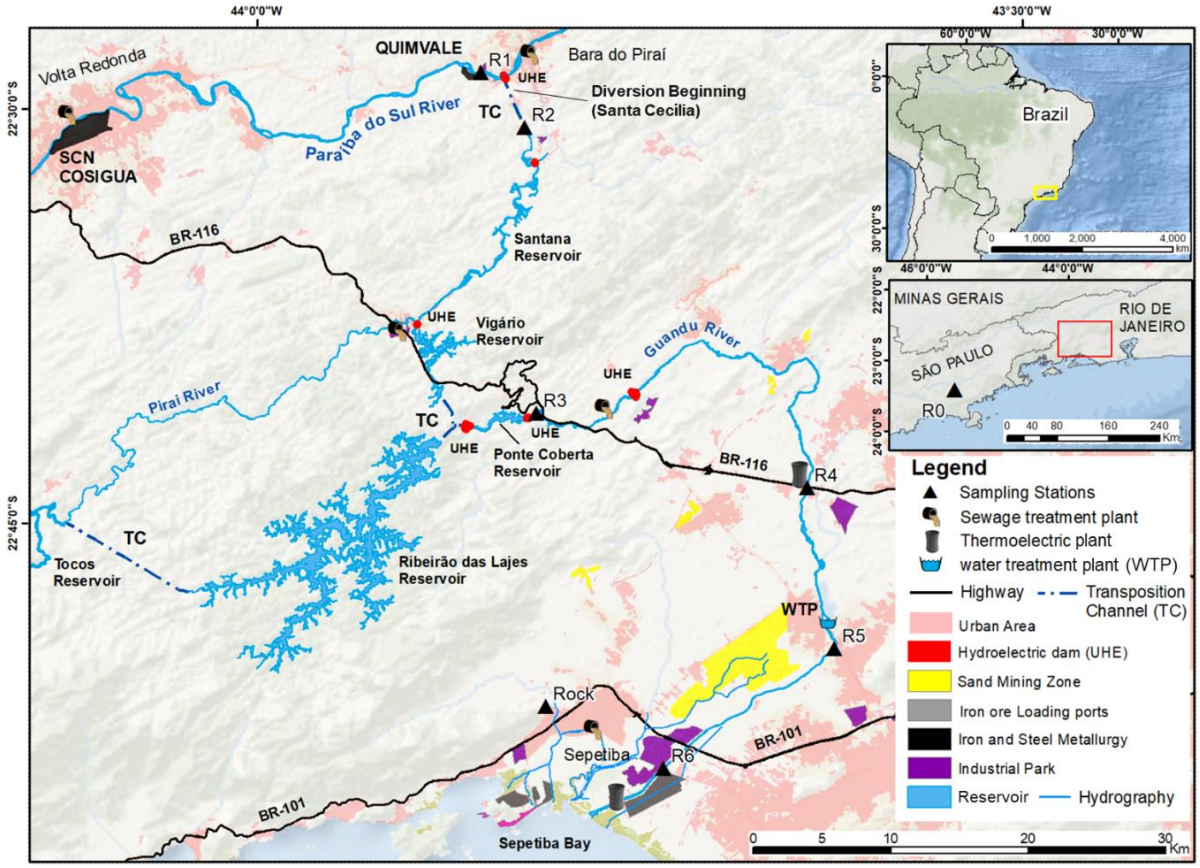

Fig. 1 Map of sampling area in the Paraíba do Sul (PSR) and Guandu Rivers (GR) highlighting the main anthropogenic activities and showing the large watershed, sampling sites (black triangles R1 to R6), and the water reservoirs.

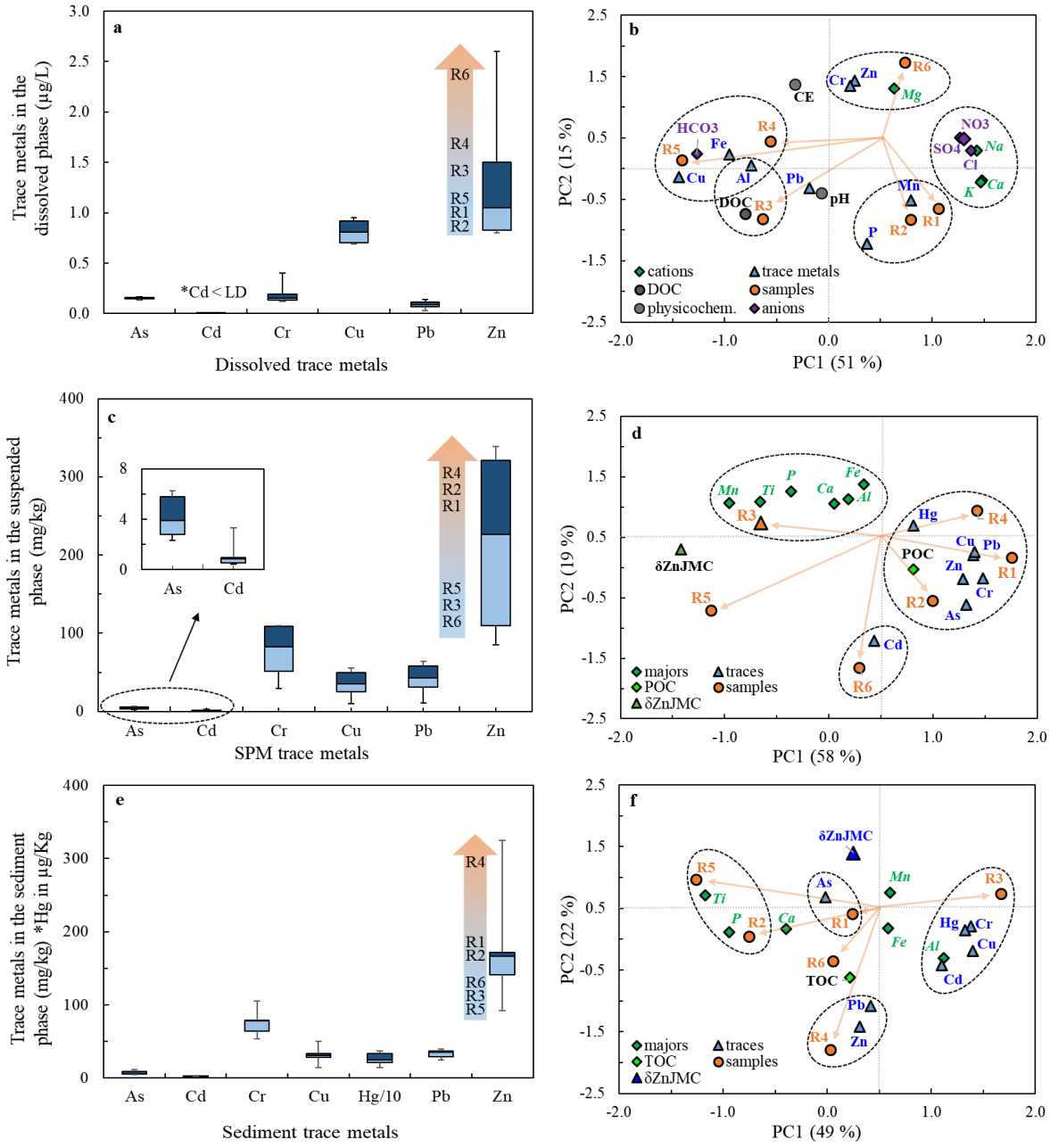

Fig. 2 Box-and-whisker plots of the trace metals concentrations (left) and Principal Component Analysis (PCA) (right) of dissolved (2a and 2b), suspended particulate material (2c and 2d), and sediment (2e and 2f) from Paraíba do Sul and Guandu Rivers (PSR-GR).

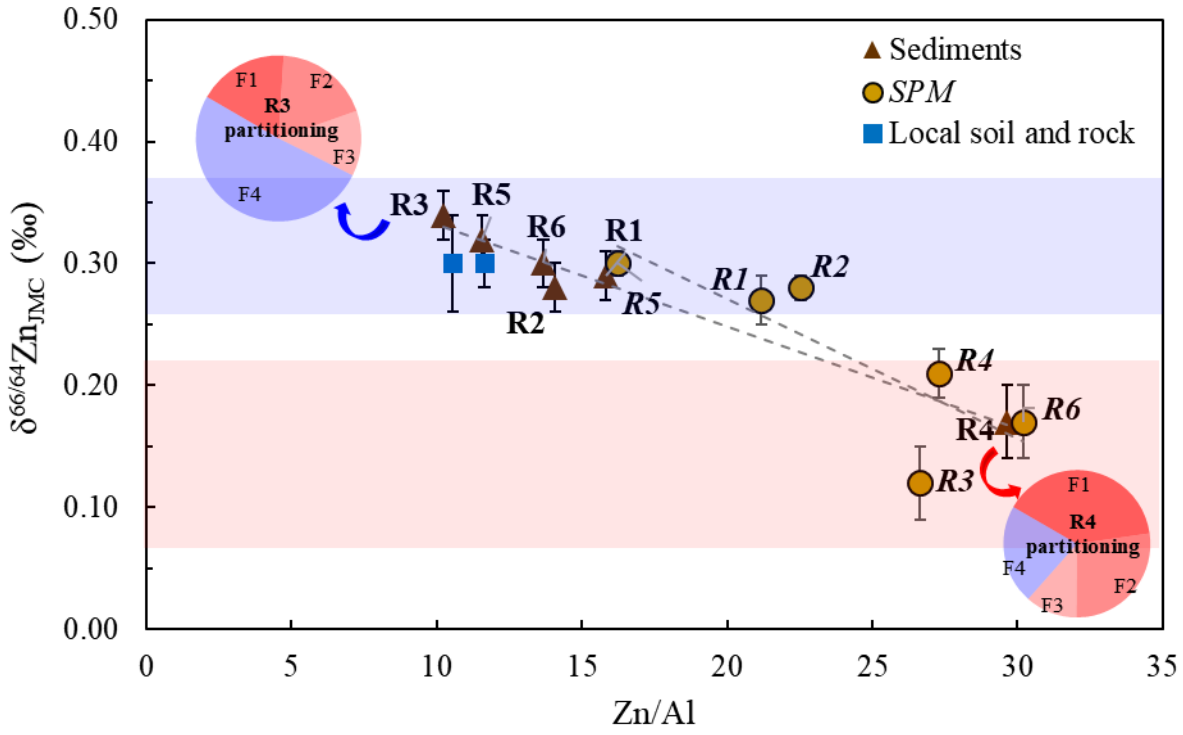

Fig. 3 A plot of the Zn isotope ratio ($\delta^{66/64}Zn_{JMC}$) versus Zn/Al in solid materials (sediment, suspended particulate matter/SPM, soil, and rock) from Paraiba do Sul and Guandu Rivers (PSR-GR). The average $\delta^{66/64}Zn_{JMC}$ values of the lithogenic end-member is represented by the light blue rectangle (+0.30 ± 0.05 ‰ is from Araújo et al. (2017a), Chen et al. (2013), Sivry et al. (2008), and Sonke et al. (2008)) and the average $\delta^{66/64}Zn_{JMC}$ values of the anthropogenic end-member is represented by the light red rectangle (+0.15 ± 0.07 ‰ is from Dong et al. (2017), John et al. (2007), Ochoa Gonzalez and Weiss (2015), Rosca et al. (2019), and Souto-Oliveira et al. (2018)). The uncertainties bars (2 s) for Zn isotopic values are given in Table 2. Pie charts represent the chemical partitioning of Zn (%) in the least contaminated (R3 - in the blue rectangle) and most anthropogenically altered (R4 – in the red rectangle) sites.

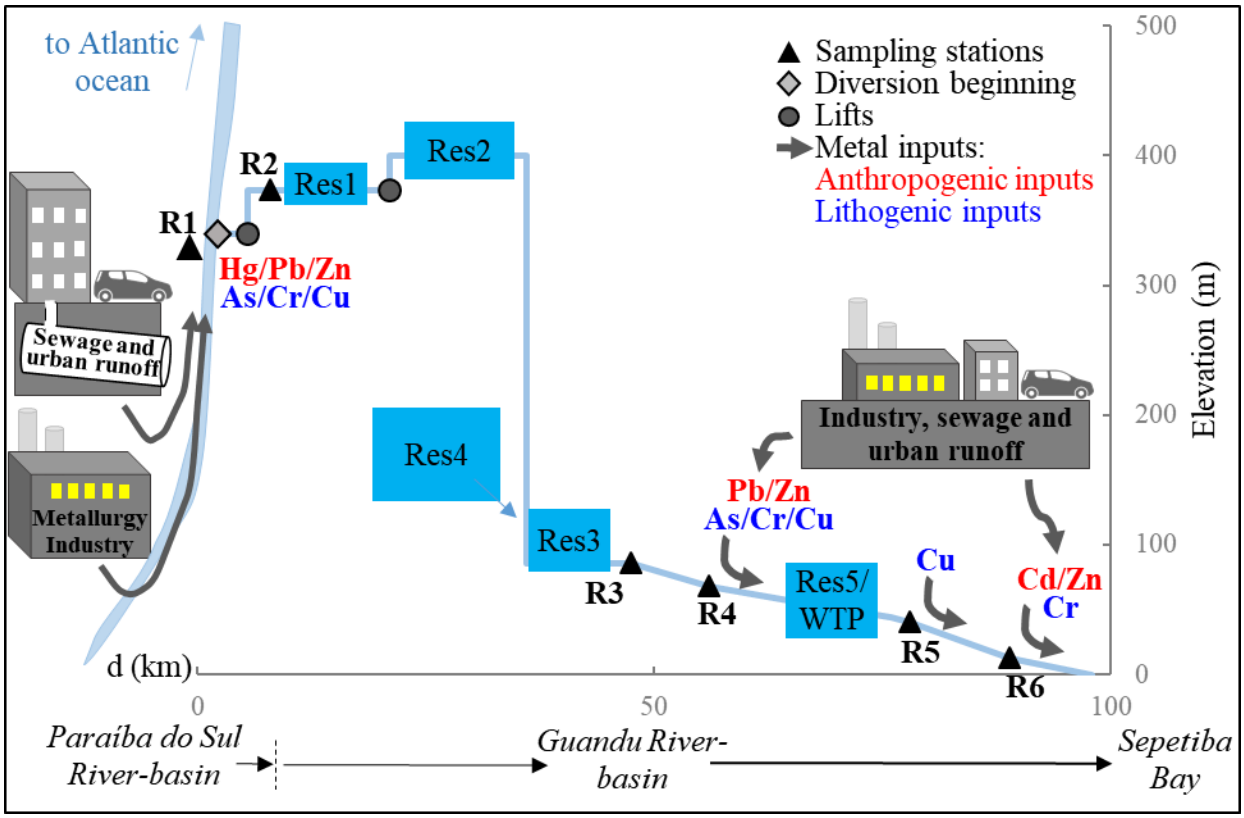

Fig. 4 Illustrative scheme of the main anthropogenic activities with the inputs of trace metals from the diverted system of Paraíba do Sul and Guandu Rivers (PSR-GR). The y and x-axis represent the elevation (m) and distances (km), respectively, in the course of the diversion system. The gray arrows represent metals inputs (dissolved and/or SPM), in which metals with red color are anthropogenic, and with blue color are lithogenic. Reservoirs: Santana (Res1), Vigário (Res2), Ponte Coberta (Res3), Lajes (Res4), and the reservoir before the Water Treatment plant - WTP (Res5).

Declaration of interests

☒ The authors declare that they have no known competing financial interests or personal relationships that could have appeared to influence the work reported in this paper.

☐The authors declare the following financial interests/personal relationships which may be considered as potential competing interests:

JOURNAL OF ENVIRONMENTAL SCIENCES

Editorial Department
P. O. Box 2871
Beijing 100085
China
Tel: 86-10-62920553
E-mail: jesc@rcees.ac.cn

Journal Publishing Agreement

Author(s): Myller S. Tonhá

Title: Trace metal dynamics in an industrialized Brazilian river: a combined application of Zn isotopes, geochemical partitioning, and multivariate statistics

The undersigned authors, with the consent of all authors, hereby assign to *Journal of Environmental Sciences*, the copyright in the above identified article to be transferred, including supplemental tables, illustrations or other information submitted in all forms and media throughout the world, in all languages and format, effective when and if the article is accepted for publication.

Authors also agree to the following terms:

A. The article submitted is not subject to any prior claim or agreement and is not under consideration for publication elsewhere.
B. The article contains no libelous or other unlawful statements and does not contain any materials that violate proprietary right of any other person, company, organization, and nation.
C. If the article was prepared jointly with other authors, the author(s) agree with the authorship sequence.

Please sign and date the document.

First Author:  Corresponding author:

Date: Brasília, 30/08/2020 Date: